

Effect of the Alkali-Metal Cation on the Bonding Mode of 2,5-Dimethylpyrrole in Divalent Samarium and Ytterbium Complexes

Mani Ganesan, Christian D. Bérubé, Sandro Gambarotta,* and Glenn P. A. Yap

Department of Chemistry, University of Ottawa, Ottawa, Ontario K1N 6N5, Canada

Received November 15, 2001

The reactions of $\text{SmI}_2(\text{THF})_2$ and $\text{YbI}_2(\text{THF})_2$ with the alkali-metal salts of 2,5-dimethylpyrrole, or the reaction of $\text{SmCl}_3(\text{THF})_3$ and $\text{YbCl}_3(\text{THF})_3$ with the same ligands followed by reduction with the appropriate alkali metals, led to the formation of divalent mono- and polynuclear complexes. Structural analysis of these complexes indicated that the bonding mode adopted by the ligand depends on the nature of the alkali-metal cation retained in the structure.

The field of organolanthanide chemistry has enjoyed a steady growth over the last two decades, a success that has been fueled by the constant discoveries of new applications and the catalytic behavior of Ln–C functionalities. Organolanthanides have been used to pursue catalytic reactions such as olefin hydrogenation,¹ hydroamination,² hydrosilylation,³ hydroboration,⁴ oligomerization,⁵ and reductive cyclization.⁶ Undeniably, the most active and versatile ligands used with lanthanide metals to perform the aforementioned transformations have been based upon the cyclopentadienyl ligand system.⁷ Furthermore, this class of ligands has also shown great versatility in stabilizing low-valent lanthanide metals such as Sm(II) and more recently even Tm(II),⁸ leading to complexes that performed spectacular transformations such as catalytic olefin polymerization,⁹ potent catalytic activity in metal-promoted

organic synthesis,¹⁰ and activation of dinitrogen¹¹ and of numerous diversified substrates.¹² In view of these processes and of the growing interest in the field, much work has been dedicated to find new ligand systems that can promote transformations similar to those observed

- (1) (a) Molander, G. A.; Hoberg, J. O. *J. Org. Chem.* **1992**, *57*, 3266. (b) Jeske, G.; Jauke, H.; Mauermann, H.; Schumann, H.; Marks, T. J. *J. Am. Chem. Soc.* **1985**, *107*, 8111. (c) Evans, W. J.; Bloom, I.; Hunter, W. E.; Atwood, J. L. *J. Am. Chem. Soc.* **1983**, *105*, 1401. (2) (a) Li, Y.; Marks, T. J. *J. Am. Chem. Soc.* **1996**, *118*, 9295. (b) Li, Y.; Marks, T. J. *Organometallics* **1996**, *15*, 3770. (c) Li, Y.; Marks, T. J. *J. Am. Chem. Soc.* **1996**, *118*, 707. (d) Gagné, M. R.; Nolan, S. P.; Marks, T. J. *Organometallics* **1990**, *9*, 1716. (3) (a) Fu, P. F.; Brard, L.; Li, Y.; Marks, T. J. *J. Am. Chem. Soc.* **1995**, *117*, 7157 and references cited therein. (b) Molander, G. A.; Julius, M. *J. Org. Chem.* **1992**, *57*, 6347. (4) (a) Bijpost, E. A.; Duchateau, R.; Teuben, J. H. *J. Mol. Catal.* **1995**, *95*, 121. (b) Harrison, K. N.; Marks, T. J. *J. Am. Chem. Soc.* **1992**, *114*, 9220. (c) Molander, G. A.; Hoberg, J. O. *J. Am. Chem. Soc.* **1992**, *114*, 3123. (5) (a) Thompson, M. E.; Bercaw, J. E. *Pure Appl. Chem.* **1984**, *56*, 1. (b) Watson, P. L. *J. Am. Chem. Soc.* **1982**, *104*, 337. (c) Parkin, G.; Bunel, E.; Burger, B. J.; Trimmer, M. S.; van Asselt, A.; Bercaw, J. E. *J. Mol. Catal.* **1987**, *41*, 21. (d) Watson, P. L.; Roe, D. C. *J. Am. Chem. Soc.* **1982**, *104*, 6471. (6) (a) Molander, G. A.; Nichols, P. J. *J. Am. Chem. Soc.* **1995**, *117*, 4415. (b) Heeres, H. J.; Heeres, A.; Teuben, J. H. *Organometallics* **1990**, *9*, 1508. (c) Piers, W. E.; Bercaw, J. E. *J. Am. Chem. Soc.* **1990**, *112*, 9406. (d) Piers, W. E.; Shapiro, P. J.; Bunel, E. E.; Bercaw, J. E. *Synlett* **1990**, *74*. (e) Qian, C.; Ge, Y.; Deng, D.; Gu, Y.; Zhang, C. *J. Organomet. Chem.* **1988**, *344*, 175. (f) Qian, C.; Zhu, D.; Li, D. *J. Organomet. Chem.* **1992**, *430*, 175. (7) See for example: (a) Marks, T. J.; Fragala, I. L. *Fundamental and Technological Aspects of Organo-f-Element Chemistry*; D. Reidel: Dordrecht, The Netherlands, 1985; (b) Schumann, H. *Angew. Chem., Int. Ed. Engl.* **1984**, *23*, 474. (c) Evans, W. J. *Polyhedron* **1987**, *6*, 803. (d) Evans, W. J. *J. Organomet. Chem.* **1983**, *250*, 217. (8) Evans, W. J.; Allen, N. T.; Ziller, J. W. *J. Am. Chem. Soc.* **2001**, *123*, 7927.

- (9) (a) Jeske, G.; Lauke, H.; Mauermann, H.; Swepston, P. N.; Schumann, H.; Marks, T. J. *J. Am. Chem. Soc.* **1985**, *107*, 8091. (b) Jeske, G.; Schock, L. E.; Swepston, P. N.; Schumann, H.; Marks, T. J. *J. Am. Chem. Soc.* **1985**, *107*, 8103. (c) Watson, P. L.; Parshall, G. W. *Acc. Chem. Res.* **1985**, *18*, 51.

- (10) (a) Schumann, H.; Meese-Marktscheffel, J. A.; Esser, L. *Chem. Rev.* **1995**, *95*, 865. (b) Edelmann, F. T. In *Comprehensive Organometallic Chemistry II*; Abel, E. W., Stone, F. G. A., Wilkinson, G., Eds.; Pergamon Press: Oxford, U.K., 1995; Vol. 4, Chapter 2 and references therein. (c) Schaverien, C. J. *Adv. Organomet. Chem.* **1994**, *36*, 283 and references therein. (d) Evans, W. J. *Adv. Organomet. Chem.* **1985**, *24*, 31 and references therein. (e) Kagan, H. B.; Namy, J. L. In *Handbook on the Physics and Chemistry of Rare Earths*; Gschneider, K. A., Eyring, L.; Elsevier: Amsterdam, 1984; Chapter 50. (f) Marks, T. J.; Ernst, R. D. In *Comprehensive Organometallic Chemistry*; Wilkinson, G., Stone, F. G. A., Abel, E. W., Eds.; Pergamon Press: Oxford, U.K., 1982; Chapter 21, and references therein.

- (11) Evans, W. J.; Ulibarri, T. A.; Ziller, J. M. *J. Am. Chem. Soc.* **1988**, *110*, 6877.

- (12) (a) Evans, W. J.; Keyer, R. A.; Rabe, G. W.; Drummond, D. K.; Ziller, J. W. *Organometallics* **1993**, *12*, 4664. (b) Evans, W. J.; Grate, J. W.; Doedens, R. J. *J. Am. Chem. Soc.* **1985**, *107*, 1671. (c) Evans, W. J.; Ulibarri, T. A. *J. Am. Chem. Soc.* **1987**, *109*, 4292. (d) Evans, W. J.; Drummond, D. K. *J. Am. Chem. Soc.* **1988**, *110*, 2772. (e) Evans, W. J.; Drummond, D. K. *Organometallics* **1988**, *7*, 797. (f) Evans, W. J.; Drummond, D. K.; Chamberlain, L. R.; Doedens, R. J.; Bott, S. G.; Zhang, H.; Atwood, J. L. *J. Am. Chem. Soc.* **1988**, *110*, 4983. (g) Evans, W. J.; Drummond, D. K. *J. Am. Chem. Soc.* **1986**, *108*, 7440. (h) Evans, W. J.; Ulibarri, T. A.; Ziller, J. W. *J. Am. Chem. Soc.* **1990**, *112*, 2314. (i) Evans, W. J.; Grate, J. W.; Hughes, L. A.; Zhang, H.; Atwood, J. L. *J. Am. Chem. Soc.* **1985**, *107*, 3728.

- (13) (a) Sen, A.; Chebolu, V.; Rheingold, A. L. *Inorg. Chem.* **1987**, *26*, 1821. (b) Evans, W. J.; Anwender, R.; Ansari, M. A.; Ziller, J. W. *Inorg. Chem.* **1995**, *34*, 5. (c) Hitchcock, P. B.; Holmes, S. A.; Lappert, M. F.; Tian, S. *J. Chem. Soc., Chem. Commun.* **1994**, 2691. (d) Biagini, P.; Lugli, G.; Abis, L.; Millini, R. *J. Organomet. Chem.* **1994**, *474*. (e) Desurmont, G.; Li, Y.; Yasuda, H.; Maruo, T.; Kanehisa, N.; Kai, Y. *Organometallics* **2000**, *19*, 1811.

- (14) (a) Chebolu, V.; Whittle, R. R.; Sen, A. *Inorg. Chem.* **1985**, *24*, 3082. (b) Evans, W. J.; Drummond, D. K.; Zhang, H.; Atwood, J. L. *Inorg. Chem.* **1988**, *27*, 575. (c) Evans, W. J.; Rabe, G. W.; Ziller, J. W.; *Inorg. Chem.* **1994**, *33*, 3072. (d) White, J. P., III; Deng, H.; Boyd, E. P.; Gallucci, J.; Shore, S. G. *Inorg. Chem.* **1994**, *33*, 1685. (e) Evans, W. J.; Rabe, G. W.; Ziller, J. W. *Organometallics* **1994**, *13*, 1641. (f) Minhas, R.; Song, J.; Ma, Y.; Gambarotta, S. *Inorg. Chem.* **1996**, *35*, 1866. (g) Evans, J. W.; Ansari, M. A.; Ziller, J. W. *Inorg. Chem.* **1996**, *35*, 5435. (h) Schaverien, C. J.; Orpen, A. G. *Inorg. Chem.* **1991**, *30*, 4968. (i) Edelmann, F. T. *Coord. Chem. Rev.* **1995**, *137*, 403. (j) Schumann, H.; Rosenthal, E. C. E.; Winterfield, J.; Kociok-Kohn, G. *J. Organomet. Chem.* **1995**, *495*, C12.

with the Cp type ligands. Alternate ligands, such as alkoxides,¹³ amides,¹⁴ phosphides,¹⁵ and pyrazolylborates,¹⁶ were successfully used to stabilize low-valent samarium, but the caliber of the transformations displayed by the samarocenes was never reproduced.

One of the recurring features in lanthanide cyclopentadienyl chemistry is the retention of alkali-metal cations and of their halide counteranions in the molecular structure. The presence of these units, expected to be inert, may occasionally affect the chemical reactivity, often affording intractable products or complicating the reaction pathways. The robustness of the lanthanide–halogen bond makes difficult the dissociation of the halogen from the lanthanide coordination sphere and is likely to be at the origin of the problem.

Our continuing studies on the polypyrrolide derivatives of low-valent samarium have highlighted a promising ability to stabilize highly reactive divalent samarium clusters.¹⁷ Even more important was the observation that the dipyrrolide systems, closely reminiscent of an *ansa*-metallocene type of ligand, are capable of substantially increasing the reactivity with respect to samarocene, since a four-electron reduction of dinitrogen was observed¹⁸ rather than labile coordination.¹¹ Therefore, since a pyrrolyl anion is closely reminiscent of the cyclopentadienyl moiety, the next obvious step was to attempt the preparation of divalent (pyrrolyl)₂Ln types of complexes for future reactivity studies. The use of 2,5-dimethylpyrrole was found to be advantageous over that of simple pyrrole, since the latter is prone to decomposition through the formation of polymeric compounds. In this first report, we wish to report the synthesis and characterization of a series of divalent Sm and Yb pyrrolide compounds and the remarkable role of the alkali-metal cation in determining the type of M–ligand bonding mode.

Experimental Section

All operations were performed under an inert atmosphere of a nitrogen-filled drybox or by using Schlenk-type glassware in combination with a nitrogen–vacuum line. Solvents were dried by passing through a column of Al₂O₃ under an inert atmosphere prior to use, degassed in vacuo, and transferred and stored under an inert atmosphere. SmI₂(THF)₂,¹⁹ SmCl₃·(THF)₃,²⁰ YbI₂(THF)₂,²¹ and YbCl₃(THF)₃²² were prepared according to literature procedures. The NaH and KH suspensions in mineral oil (Aldrich) were washed with hexane, dried, and stored under nitrogen in sealed ampules. THF-*d*₈ was

dried over Na/K alloy, vacuum-transferred into ampules, and stored under nitrogen prior to use. 2,5-Dimethylpyrrole and the solutions of *n*-BuLi and CH₃Li (Aldrich) were used as received. NMR spectra were recorded on a Varian Gemini 200 and on a Bruker AMX-500 spectrometer using vacuum-sealed NMR tubes prepared inside a drybox. Infrared spectra were recorded on a Mattson 3000 FTIR instrument from Nujol mulls prepared inside a drybox. Samples for magnetic susceptibility measurements were carried out at room temperature using a Gouy balance (Johnson Matthey) and corrected for underlying diamagnetism. Elemental analyses were carried out using a Perkin-Elmer Series II CHN/O 2400 analyzer.

Synthesis of {(μ - η^1 : η^5 -Me₂C₄H₂N)₃Sm(μ -Cl)[Li(THF)₂]₂} (1). A solution of 2,5-dimethylpyrrole (1.3 mL, 12.8 mmol) in THF (40 mL) was stirred with *n*-BuLi (1.6 M, 8.5 mL, 13.6 mmol) at room temperature for 30 min. Subsequent addition of SmCl₃(THF)₃ (3.0 g, 6.4 mmol) in THF resulted in an immediate color change to orange. After the reaction mixture was stirred for 24 h, metallic lithium (0.045 g, 6.4 mmol) was added under an argon atmosphere. Within 1 h, the color changed to dark brown and the mixture was stirred for an additional 24 h to ensure that all the lithium was consumed. The solvent was evaporated under vacuum, and the residue was extracted with ether, after which the solution was centrifuged to remove an insoluble precipitate. The ether was removed in vacuo to give a powder, which was solubilized in THF (10 mL). Hexane (20 mL) was added to the solution, which led to the crystallization of **1** after 3 days at –36 °C (2.8 g, 3.6 mmol, 56% yield). Anal. Calcd (found) for C₃₄H₅₆N₃O₄·ClLi₂Sm: C, 53.00 (52.88); H, 7.33 (7.08); N, 5.45 (5.12). IR (Nujol, cm⁻¹): ν 3070 (m), 2726 (w), 1501 (m), 1310 (m), 1294 (m), 1261 (m), 1042 (vs), 961 (w), 914 (s), 895 (s), 757 (vs), 723 (w), 669 (w), 601 (m). $\mu_{\text{eff}} = 3.3 \mu_{\text{B}}$.

Synthesis of {(μ - η^1 : η^5 -Me₂C₄H₂N)₃Sm(μ -I)[Li(TMEDA)₂]-[Li(OEt)₂]}(ether)_{0.5} (2). A solution of SmI₂(THF)₂ (2.9 g, 4.4 mmol) in THF (100 mL) was treated with 3 equiv of lithium 2,5-dimethylpyrrole (1.3 g, 13.3 mmol), resulting in an instantaneous color change to deep purple. After the mixture was stirred for 2 h, the solvent was removed in vacuo, and the dark purple residue was redissolved in ether (75 mL). Upon addition of TMEDA (2.0 mL, 13.2 mmol) an appreciable amount of white solid precipitated. After it stood at room temperature for 4 h, the solution was filtered and concentrated to 30 mL. Standing at room temperature overnight yielded purple plates of **2** (2.2 g, 2.7 mmol, 61% yield). Anal. Calcd (found) for C₃₀H₅₅N₅O_{1.5}Li₂I₂Sm: C, 44.99 (44.58); H, 6.92 (6.84); N, 8.74 (8.63). IR (Nujol mull, cm⁻¹): ν 3087 (w), 2724 (w), 1501 (w), 1459 (vs), 1376 (vs), 1288 (m), 1266 (m), 1159 (m), 1129 (m), 1031 (s), 946 (s), 792 (s), 761 (vs). $\mu_{\text{eff}} = 3.2 \mu_{\text{B}}$.

Synthesis of {[(Na(THF)₂)(μ - η^1 : η^5 -Me₂C₄H₂N)₂Sm]₂(μ - η^1 : η^5 -Me₂C₄H₂N)₂}(THF)₂ (3). A solution of 2,5-dimethylpyrrole (1.1 mL, 1.1 g, 11.2 mmol) in THF (40 mL) was stirred with NaH (0.3 g, 11.6 mmol) at room temperature for 30 min. Subsequent addition of SmCl₃(THF)₃ (1.8 g, 3.7 mmol) in THF and reflux for 20 h resulted in a yellow solution. After addition of finely dispersed sodium (0.09 g, 3.9 mmol) the solution was stirred for 7 days, affording a dark brown solution. The solution was centrifuged and concentrated to 20 mL. Red-brown crystals of **3** were obtained upon cooling the solution to 4 °C (1.3 g, 1.0 mmol, 54% yield). Anal. Calcd (found) for C₆₀H₉₆N₆Na₂O₆Sm₂: C, 53.61 (53.62); H, 7.20 (7.02); N, 6.25 (6.11). IR (Nujol, cm⁻¹): ν 3084 (m), 3066 (m), 2729 (w), 1500 (w), 1308 (w), 1290 (w), 1258 (s), 1171 (w), 1096 (w), 1051 (vs), 1033 (vs), 960 (w), 892 (w), 800 (w), 763 (vs), 739 (s), 702 (w). $\mu_{\text{eff}} = 2.3 \mu_{\text{B}}$.

Isolation of {(μ - η^1 : η^5 -Me₂C₄H₂N)₂Yb(μ -Cl)[Li(OEt)₂]}₂ (4) and {[(μ - η^1 : η^5 -Me₂C₄H₂N)₂Yb(μ -Cl)][Li(THF)(OEt)₂]-[μ -Cl]Li(OEt)₂]}₂ (5). A solution of 2,5-dimethylpyrrole (0.9 g, 0.95 mL, 9.4 mmol) in THF (40 mL) was stirred with *n*-BuLi (1.6 M, 5.9 mL, 9.4 mmol) at room temperature for 30 min. Subsequent addition of YbCl₃(THF)₃ (2.3 g, 4.7 mmol) in THF

(15) (a) Nief, F.; Ricard, L. *J. Organomet. Chem.* **1994**, *464*, 149. (b) Rabe, G.; Riede, J.; Schier, A. *Inorg. Chem.* **1996**, *35*, 2680. (c) Gosink, H. J.; Nief, F.; Ricard, L.; Mathey, F. *Inorg. Chem.* **1995**, *34*, 1306. (d) Fryzuk, M. D.; Haddad, T. S.; Rettig, S. J. *Organometallics* **1992**, *11*, 2967.

(16) (a) Takats, J. *J. Alloys Compd.* **1997**, *249*, 52; (b) Hasinoff, L.; Takats, J.; Zhang, X. W.; Bond, A. H.; Rogers, R. D. *J. Am. Chem. Soc.* **1994**, *116*, 8833. (c) Ferrence, G. M.; McDonald, R.; Takats, J. *Angew. Chem., Int. Ed.* **1999**, *38*, 2233.

(17) Ganesan, M.; Gambarotta, S.; Yap, G. P. A. *Angew. Chem., Int. Ed. Engl.* **2001**, *113*, 788.

(18) Dubé, T.; Conoci, S.; Gambarotta, S.; Yap, G. P. A.; Vasapollo, G. *Angew. Chem., Int. Ed.* **1999**, *38*, 3657.

(19) Evans, W. J.; Grate, J. W.; Choi, H. W.; Bloom, I.; Hunter, W. E.; Atwood, J. L. *J. Am. Chem. Soc.* **1985**, *107*, 941.

(20) Anhydrous SmCl₃ was prepared by following a standard procedure: (a) Freeman, J. H.; Smith, M. L. *J. Inorg. Nucl. Chem.* **1958**, *7*, 224. This compound was transformed into the corresponding tetrahydrofuranate: (b) Manzer, L. E., *Inorg. Synth.* **1982**, *21*, 135.

(21) Watson, P. L.; Tulip, T. H.; Williams, I. *Organometallics* **1990**, *9*, 1999.

(22) Angelici, R. J. *Inorg. Synth.* **1990**, *27*, 136.

caused the solution to turn orange. After the reaction mixture was stirred for 24 h, metallic lithium (0.033 g, 4.7 mmol) was added under an argon atmosphere and stirring continued for 4 days to give a yellow solution. The solvent was evaporated in vacuo, and the resulting residue was extracted with ether (40 mL), affording a red solution. The solution was centrifuged to remove insoluble LiCl and was then concentrated to 20 mL and cooled to $-36\text{ }^{\circ}\text{C}$ for 4 days, affording red crystals of **4** (0.9 g, 0.94 mmol, 40% yield). Anal. Calcd (found) for $\text{C}_{32}\text{H}_{52}\text{Cl}_2\text{Li}_2\text{N}_4\text{O}_2\text{Yb}_2$ (**4**): C, 40.22 (38.61); H, 5.48 (5.14); N, 5.86 (5.81). IR (Nujol, cm^{-1}): ν 3090 (m), 3075 (m), 2729 (m), 1309 (m), 1255 (m), 1195 (w), 1154 (m), 1089 (m), 1057 (m), 1033 (s), 1002 (m), 963 (w), 905 (w), 840 (w), 791 (w), 763 (vs), 723 (m), 669 (w), 601 (m). ^1H NMR (200 MHz, THF- d_6 , $22\text{ }^{\circ}\text{C}$): δ 1.11 (t, 12H, CH₃), 2.17 (br s, 24H, CH₃), 3.37 (q, 8H, CH₂), 5.80 (br s, 8H, CH). ^{13}C NMR (125.76 MHz, THF- d_6 , $22\text{ }^{\circ}\text{C}$): δ 15.65 (CH₃), 16.68 (CH₃), 17.75 (CH₃), 66.30 (CH₂ ether), 108.26 (CH pyrrole), 110.06 (CH pyrrole), 135.29 (quaternary C pyrrole). The mother liquor was cooled again for 4 days, affording yellow crystals of **5** along with red crystals of **4**. Characterization of **5** was therefore restricted to X-ray crystallography.

Synthesis of $\{(\mu\text{-}\eta^1\text{-}\eta^5\text{-Me}_2\text{C}_4\text{H}_2\text{N})_2\text{Yb}(\mu\text{-D})_2[\text{Li}(\text{THF})]_2\}_2\text{-}(\text{toluene})_n$ (**6**). A solution of 2,5-dimethylpyrrole (0.4 g, 0.45 mL, 4.4 mmol) in THF (20 mL) was stirred with CH₃Li (1.4 M, 3.1 mL, 4.4 mmol) at room temperature for 30 min. Subsequent addition of YbI₂(THF)₂ (1.2 g, 2.2 mmol) in THF (30 mL) resulted in an immediate color change to orange. The mixture was stirred for an additional 24 h. The solvent was evaporated in vacuo, the residue was extracted with toluene (30 mL), and the heterogeneous solution was centrifuged. Red crystals of **6** were formed upon allowing the solution to stand for 5 days at room temperature (1.0 g, 0.6 mmol, 55% yield). Anal. Calcd (found) for $\text{C}_{47}\text{H}_{72}\text{Li}_4\text{Li}_4\text{N}_4\text{O}_4\text{Yb}_2$: C, 34.45 (34.42); H, 4.43 (4.15); N, 3.42 (3.69). IR (Nujol, cm^{-1}): ν 3084 (w), 2736 (w), 1634 (w), 1603 (w), 1548 (w), 1342 (s), 1312 (s), 1294 (s), 1259 (vs), 1197 (w), 1174 (w), 1081 (w), 1037 (vs), 962 (s), 915 (vs), 890 (vs), 783 (vs), 734 (vs), 696 (s), 670 (w), 636 (w), 603 (s). ^1H NMR (200 MHz, THF- d_6 , $22\text{ }^{\circ}\text{C}$): δ 1.73 (m, 4H, THF), 2.18 (br s, 6H, CH₃), 3.59 (m, 4H, THF), 5.77 (br s, 2H, CH). ^{13}C NMR (125.76 MHz, THF- d_6 , $22\text{ }^{\circ}\text{C}$): δ 17.30 (CH₃ pyrrole), 26.30 (CH₂ THF), 68.32 (CH₂ THF), 108.52 (CH pyrrole), 135.50 (quaternary C pyrrole).

Synthesis of $\{(\mu\text{-}\eta^1\text{-}\eta^5\text{-Me}_2\text{C}_4\text{H}_2\text{N})_4[\text{K}(\text{THF})]_2\text{Yb}\}_n$ (**7**). A solution of 2,5-dimethylpyrrole (0.4 g, 4.6 mmol) in THF (25 mL) was stirred with KH (0.2 g, 4.7 mmol) at room temperature for 30 min. Subsequent addition of YbI₂(THF)₂ (1.3 g, 2.3 mmol) in THF (30 mL) resulted in a color change to yellow-orange while the solution was stirred for 20 h. The solution was centrifuged to remove KI and then concentrated to a small volume (15 mL). Yellow crystals of **7** were obtained upon layering hexane over the solution (0.8 g, 1.0 mmol, 43% yield). IR (Nujol, cm^{-1}): ν 3064 (w), 2729 (w), 2360 (w), 2342 (w), 1307 (w), 1257 (s), 1096 (w), 1036 (s), 955 (w), 913 (w), 801 (w), 754 (s), 739 (s). ^1H NMR (200 MHz, THF- d_6 , $22\text{ }^{\circ}\text{C}$): δ 1.68 (br s, 4H, THF), 2.42 (br s, 12H, CH₃), 3.54 (br s, 4H, THF), 5.53 (br s, 4H, CH). ^{13}C NMR (125.76 MHz, THF- d_6 , $22\text{ }^{\circ}\text{C}$): δ 16.70 (CH₃ pyrrole), 26.40 (CH₂ THF), 68.20 (CH₂ THF), 105.70 (CH pyrrole), 133.20 (quaternary C pyrrole).

Structural Determination. Suitable crystals were selected, mounted on thin glass fibers using viscous oil, and cooled to the data collection temperature. Data were collected on a Bruker AX SMART 1k CCD diffractometer using 0.3° ω -scans at 0, 90, and 180° in ϕ . Unit-cell parameters were determined from 60 data frames collected at different sections of the Ewald sphere. Semiempirical absorption corrections based on equivalent reflections were applied to the data.²³

No symmetry higher than triclinic was evident from the diffraction data of **1**, **2**·0.5(ether), and **6**·(toluene). Solution in

Table 1. Crystal Data and Structure Analysis Results for Samarium Complexes

	1	2	3
formula	$\text{C}_{34}\text{H}_{56}\text{ClLi}_2\text{-N}_3\text{O}_4\text{Sm}$	$\text{C}_{30}\text{H}_{55}\text{ILi}_2\text{-N}_5\text{O}_{1.5}\text{Sm}$	$\text{C}_{60}\text{H}_{96}\text{N}_6\text{-Na}_2\text{O}_6\text{Sm}_2$
fw	770.50	800.92	1344.11
space group	triclinic, $P\bar{1}$	monoclinic, $P2_1/c$	triclinic, $P\bar{1}$
<i>a</i> (Å)	11.307(4)	21.147(1)	11.564(2)
<i>b</i> (Å)	13.137(5)	10.1298(5)	16.366(3)
<i>c</i> (Å)	17.091(6)	19.766(1)	19.305(4)
α (deg)	89.778(4)	90	64.990(3)
β (deg)	81.829(4)	117.247(1)	80.609(3)
γ (deg)	66.946(4)	90	78.348(3)
<i>V</i> (Å ³)	2308(1)	3764.4(3)	3230(1)
<i>Z</i>	2	4	2
radiation (K α , Å)	0.710 73	0.710 73	0.710 73
<i>F</i> (000)	796	1384	1612
<i>T</i> (K)	173(2)	203(2)	203(2)
<i>D</i> _{calcd} (Mg m ⁻³)	1.108	1.382	1.413
μ _{calcd} (mm ⁻¹)	1.360	1.863	2.408
R1, wR2 ^a	0.0824, 0.2028	0.0488, 0.1083	0.0422, 0.1022
GOF	1.013	1.052	1.030

$$^a \text{R1} = \sum |F_o - F_c| / \sum F_o; \text{wR2} = [\sum (F_o^2 - F_c^2)^2 / \sum (wF_o^2)^2]^{1/2}.$$

the centric option yielded chemically reasonable and computationally stable results of refinement. Systematic absences in the diffraction data and unit-cell parameters were uniquely consistent for the reported space groups for **3**·2(THF), **4**, **5**, and **7**. The structures were solved by direct methods, completed with difference Fourier syntheses, and refined with full-matrix least-squares procedures based on F^2 . The absolute configuration parameter in **7** was refined to nil, indicating that the true hand of the data had been determined.

Two symmetry unique but chemically identical molecules of **2** are located, each at an inversion center. The compound molecule for **5** is located at an inversion center. Compounds **6**·(toluene) and **7** are infinite polymers propagated by inversion and by 2-fold rotation, respectively. The coordinated solvent in **5** was resolved to be diethyl ether/THF with a site occupancy distribution of 60/40. A toluene solvent molecule was located cocrystallized at half-occupancy at an inversion center of **6**·(toluene). Two molecules of tetrahydrofuran solvent were found in the asymmetric unit of **2**·0.5(ether). A molecule of diethyl ether solvent was found rotationally disordered along its molecular axis at half-occupancy at an inversion center in **3**·2(THF). All noncoordinated, cocrystallized molecules were refined isotropically with cyclic molecules refined as flat polygons. All other non-hydrogen atoms were refined with anisotropic displacement parameters. All hydrogen atoms were treated as idealized contributions. All scattering factors and anomalous dispersion factors are contained in the SHELXTL 5.10 program library.

Crystal data and structure analysis results for the samarium and ytterbium complexes are given in Tables 1 and 2, respectively.

Results and Discussion

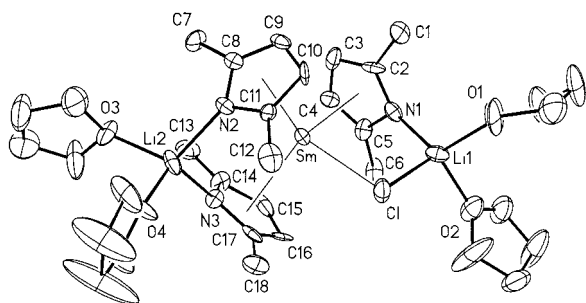
Treatment of $\text{SmCl}_3(\text{THF})_3$ with 2 equiv of the lithium salt of 2,5-dimethylpyrrole followed by reduction using metallic lithium under an argon atmosphere in THF afforded $\{(\mu\text{-}\eta^1\text{-}\eta^5\text{-Me}_2\text{C}_4\text{H}_2\text{N})_3\text{Sm}(\mu\text{-Cl})[\text{Li}(\text{THF})_2]_2\}$ (**1**) in 57% yield. The dark color observed for this compound is indicative of a divalent samarium atom, an observation that was further validated by the X-ray crystal determination, analytical data, and magnetic moment.

The complex (Figure 1; bond distances and angles are given in Table 3) consists of a divalent Sm center surrounded by three π -bonded 2,5-dimethylpyrrole frag-

Table 2. Crystal Data and Structure Analysis Results for Ytterbium Complexes

	4	5	6	7
formula	C ₃₂ H ₅₂ Cl ₂ Li ₂ N ₄ O ₂ Yb ₂	C ₄₈ H ₈₄ Cl ₄ Li ₄ N ₄ O ₆ Yb ₂	C ₄₇ H ₇₂ I ₄ Li ₄ N ₄ O ₄ Yb ₂	C ₃₂ H ₄₈ K ₂ N ₄ O ₂ Yb
fw	955.64	1331.22	1638.58	771.98
space group	monoclinic, <i>P2</i> ₁ / <i>c</i>	monoclinic, <i>P2</i> ₁ / <i>c</i>	triclinic, <i>P</i> $\bar{1}$	orthorhombic, <i>P2</i> ₁ 2 ₁ 2
<i>a</i> (Å)	11.475(2)	11.972(2)	9.0560(9)	11.244(2)
<i>b</i> (Å)	11.541(2)	11.064(2)	11.162(1)	15.124(2)
<i>c</i> (Å)	15.711(3)	23.357(3)	15.354(2)	10.302(2)
α (deg)	90	90	77.044(2)	90
β (deg)	109.508(3)	99.980(3)	86.608(2)	90
γ (deg)	90	90	76.605(2)	90
<i>V</i> (Å ³)	1961.3(6)	3047.1(8)	1471.4(3)	1752.0(4)
<i>Z</i>	2	2	2	2
radiation (K α , Å)	0.710 73	0.710 73	0.710 73	0.710 73
<i>F</i> (000)	936	1341	778	784
<i>T</i> (K)	203(2)	203(2)	203(2)	203(2)
<i>D</i> _{calcd} (Mg m ⁻³)	1.618	1.451	1.849	1.463
μ _{calcd} (mm ⁻¹)	4.905	3.269	5.296	2.938
R1, wR2 ^a	0.0536, 0.1214	0.0402, 0.0722	0.0424, 0.0990	0.0343, 0.0510
GOF	1.022	1.056	1.007	1.020

$$^a R1 = \sum |F_o - F_c| / \sum F_o; wR2 = [\sum (F_o^2 - F_c^2)^2 / \sum (wF_o^2)^2]^{1/2}.$$

**Figure 1.** Thermal ellipsoid plot of **1**. Thermal ellipsoids are drawn at the 30% probability level.

ments (Sm–N(1)_{centroid} = 2.733(14) Å; Sm–N(2)_{centroid} = 2.701(14) Å; Sm–N(3)_{centroid} = 2.707(14) Å) and by a chlorine atom (Sm–Cl = 2.891(4) Å). If each pyrrole ring centroid is regarded as occupying a single coordination site, the coordination geometry around the Sm atom can be considered as distorted tetrahedral (Cl–Sm–N(1)_{centroid} = 97.1(7)°; Cl–Sm–N(2)_{centroid} = 100.5(7)°; Cl–Sm–N(3)_{centroid} = 101.6(7)°). Two lithium atoms are also part of the structure. The first is σ -bonded to two pyrrolide ligand N atoms (Li(2)–N(2) = 2.116(3) Å; Li(2)–N(3) = 2.047(4) Å), while the second is attached to a single pyrrolide ligand N atom (Li(1)–N(1) = 2.064(3) Å) and to the chlorine (Li(1)–Cl = 2.327(3) Å). Each lithium atom is also coordinated to two THF molecules (Li(1)–O(1) = 1.964(3) Å) and adopts a distorted-tetrahedral geometry (Cl–Li(1)–N(1) = 104.0(17)°; Cl–Li(1)–O(1) = 109.4(17)°; Cl–Li(1)–O(2) = 107.8(17)°).

The bonding mode of the pyrrolide ligands is in line with that observed in the dipyrrolide complexes of divalent samarium. However, in these particular derivatives the metal usually sustains two π -bonds and two σ -bonds, as opposed to the three π -bonds observed in **1**. Thus, to evaluate the role of the residual chlorine atom in determining the structure of the complex, a similar reaction was carried out with SmI₂(THF)₂ and 3 equiv of the lithium salt of 2,5-dimethylpyrrole. The reaction was carried out at room temperature, in THF, and in the presence of TMEDA/ether, yielding a crystalline material that was identified by X-ray crystallography as $\{(u-\eta^1:\eta^5\text{-Me}_2\text{C}_4\text{H}_2\text{N})_3\text{Sm}(u\text{-I})[\text{Li}(\text{TMEDA})_2][\text{Li}(\text{OEt}_2)_2]\}(\text{ether})_{0.5}$ (**2**) (Figure 2). Analytical and

magnetic data were in good agreement with the proposed formulation.

Besides the solvation of the Li atom (Li(1)–N(4) = 2.518(9) Å; Li(1)–N(5) = 2.179(10) Å) and the replacement of chlorine by iodine (Sm–I = 3.246(5) Å; I–Sm–N(1)_{centroid} = 98.0(14) Å; I–Sm–N(2)_{centroid} = 103.7(14) Å; I–Sm–N(3)_{centroid} = 101.0(14) Å), the structure of **2** is very similar to that of **1**. The samarium atom still adopts a similarly distorted pseudo-tetrahedral geometry, and it seems that the halide replacement of chlorine with iodine did not cause a significant structural modification.

Although the nature of the halide ion does not affect the coordination geometry of the lanthanide, the alkali-metal cation does have a large impact. Treatment of SmCl₃(THF)₃ with 3 equiv of the sodium salt of 2,5-dimethylpyrrole followed by reduction with metallic sodium in THF afforded the new complex $\{[(\text{Na}(\text{THF})_2)(u-\eta^1:\eta^5\text{-Me}_2\text{C}_4\text{H}_2\text{N})_2\text{Sm}]_2(u-\eta^1:\eta^5\text{-Me}_2\text{C}_4\text{H}_2\text{N})_2\}(\text{THF})_2$ (**3**) in 54% yield. Again, the dark red-brown of the crystals indicates the presence of divalent samarium atoms. The analytical data and magnetic moment were consistent with the formulation, as provided by the X-ray crystal structure (Figure 3). The complex is a symmetry-generated dimer where two samarium atoms are bridged by two σ - π -bonded pyrrolide rings. Each samarium atom is coordinated to four 2,5-dimethylpyrrolyl units, two of which are σ -bonded (Sm(1)–N(3) = 2.602(9) Å; Sm(1)–N(1A) = 2.623(8) Å) and two π -coordinated (Sm(1)–N(1)_{centroid} = 2.675(12) Å; Sm(1)–N(2)_{centroid} = 2.651(12) Å). Two sodium atoms, both σ - and π -bonded to 2,5-dimethylpyrrole ligands (Na(1)–N(2) = 2.385(11) Å; Na(1)–N(3)_{centroid} = 2.543(14) Å) are located toward the exterior of the molecule and complete the structure. Each Na atom is coordinated to two THF molecules (Na(1)–O(1) = 2.347(11) Å; Na(1)–O(2) = 2.307(10) Å).

The bonding around each samarium is very similar to that observed in complexes containing dipyrrolide-based ligands with the same bent-metallocene type of structure, which are precursors to dinitrogen fixation and reduction.¹⁴ Thus, it is at least surprising that this complex does not react with N₂, given the identical coordination environment. This behavior reaffirms that

Table 3. Selected Bond Distances (Å) and Angles (deg) for Samarium Complexes

1		2		3	
Sm–N(1)cent ^a	2.733(14)	Sm–N(1)cent	2.656(5)	Sm(1)–N(1A)	2.623(8)
Sm(1)–N(1A)	2.623(8)	Sm–N(2)cent	2.705(5)	Sm(1)–N(1)cent	2.675(12)
Sm–N(3)cent	2.707(14)	Sm–N(3)cent	2.678(5)	Sm(1)–N(2)cent	2.651(12)
Sm–Cl	2.891(4)	Sm–I	3.246(5)	Sm(1)–N(3)	2.602(9)
Li(1)–N(1)	2.064(3)	Li(1)–I	2.873(9)	Na(1)–O(1)	2.347(11)
Li(1)–C(1)	2.327(3)	Li(1)–N(1)	2.016(9)	Na(1)–O(2)	2.307(10)
Li(1)–O(1)	1.964(3)	Li(1)–N(4)	2.158(9)	Na(1)–N(1)	2.385(11)
Li(1)–O(2)	2.026(3)	Li(1)–N(5)	2.179(10)	Na(1)–N(3)	2.543(14)
Li(2)–N(2)	2.116(3)	Li(2)–N(2)	2.095(13)		
L(2)–N(3)	2.047(4)	Li(2)–N(3)	1.966(13)		
		Li(2)–O(1)	1.901(12)		
Cl–Sm–N(1)cent	97.1(7)	I–Sm–N(1)cent	98.0(14)	N(3)–Sm(1)–N(1A)	98.7(3)
Cl–Sm–N(2)cent	100.5(7)	I–Sm–N(2)cent	103.7(14)	N(3)–Sm(1)–N(1)cent	119.6(4)
Cl–Sm–N(3)cent	101.6(7)	I–Sm–N(3)cent	101.0(14)	N(3)–Sm(1)–N(2)cent	102.2(4)
Cl–Li(1)–N(1)	104.0(17)	I–Li(1)–N(1)	96.3(3)	O(1)–Na(1)–O(2)	91.0(4)
Cl–Li(1)–O(1)	109.4(17)	I–Li(1)–N(4)	105.5(4)	O(1)–Na(1)–N(2)	117.0(4)
Cl–Li(1)–O(2)	107.8(17)	I–Li(1)–N(5)	114.4(3)	O(1)–Na(1)–N(3)cent	115.4(4)
		O(1)–Li(2)–N(2)	126.9(7)		
		O(1)–Li(2)–N(3)	126.0(7)		

^a cent denotes a bond length or angle calculated from the ring centroid.

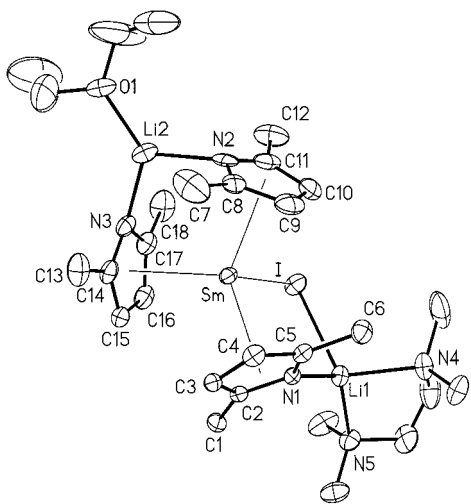


Figure 2. Thermal ellipsoid plot of **2**. Thermal ellipsoids are drawn at the 30% probability level.

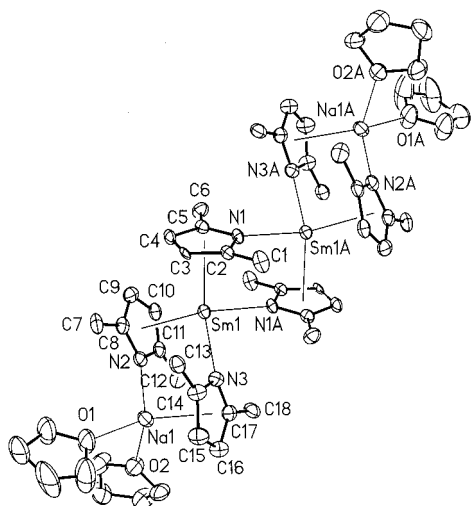


Figure 3. Thermal ellipsoid plot of **3**. Thermal ellipsoids are drawn at the 30% probability level.

the retention of the alkali-metal cation used to pursue the reaction has a substantial impact on the reaction pathway and on the metal redox potential.

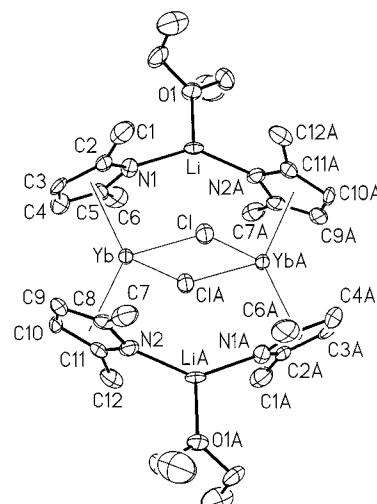


Figure 4. Thermal ellipsoid plot of **4**. Thermal ellipsoids are drawn at the 30% probability level.

The same behavior was also observed with low-valent ytterbium. Reaction of $\text{YbCl}_3(\text{THF})_3$ with 2 equiv of the lithium salt of 2,5-dimethylpyrrole followed by reduction with metallic lithium afforded a mixture of two diamagnetic Yb(II) compounds: the orange $\{(\mu\text{-}\eta^1\text{:}\eta^5\text{-Me}_2\text{C}_4\text{H}_2\text{N})_2\text{Yb}(\mu\text{-Cl})[\text{Li}(\text{OEt}_2)]\}_2$ (**4**) and the yellow $\{[(\mu\text{-}\eta^1\text{:}\eta^5\text{-Me}_2\text{C}_4\text{H}_2\text{N})_2\text{Yb}(\mu\text{-Cl})][\text{Li}(\text{THF})(\text{OEt}_2)][(\mu\text{-Cl})\text{Li}(\text{OEt}_2)]\}_2$ (**5**). Complex **4** was characterized through elemental analysis, ^1H NMR, and ^{13}C NMR, all of which supported the structure shown by X-ray crystallography (Figure 4; bond distances and angles are given in Table 4). The complex is dimeric with two divalent ytterbium centers bridged by two chlorine atoms ($\text{Yb}\text{-Cl} = 2.711(3)$ Å; $\text{Yb}\text{-Cl(A)} = 2.688(3)$ Å). Each ytterbium is also π -bonded to two 2,5-dimethylpyrrole ligands ($\text{Yb}\text{-N(1)}_{\text{centroid}} = 2.459(15)$ Å; $\text{Yb}\text{-N(2)}_{\text{centroid}} = 2.456(15)$ Å). The structure also contains two lithium atoms that are σ -bonded to two pyrrole ligands ($\text{Li}\text{-N(1)} = 2.020(2)$ Å; $\text{Li}\text{-N(2A)} = 1.980(2)$ Å), each bearing one molecule of ether ($\text{Li}\text{-O(1)} = 1.870(2)$ Å).

While complex **4** was isolated from the reaction mixture as an analytically pure crystalline solid, complex **5** was obtained as a minor product of a second crop

Table 4. Selected Bond Distances (Å) and Angles (deg) for Yb Complexes

4		5		6		7	
Yb–Cl	2.711(3)	Yb–N(1)cent	2.469(10)	Yb–N(1)cent	2.440(7)	Yb–N(1)	2.378(4)
Yb–Cl(A)	2.688(3)	Yb–N(2)cent	2.454(10)	Yb–N(2)cent	2.450(7)	Yb–N(2)	2.409(4)
Yb–N(1)cent ^a	2.459(15)	Yb–Cl(1)	2.682(3)	Yb–I(1)	3.1203(5)	Yb–N(1C)	2.378(4)
Yb–N(2)cent	2.456(15)	Yb–Cl(2)	2.744(2)	Yb–I(2)	3.1174(5)	Yb–N(2C)	
Li–O(1)	1.870(2)	Li(1)–Cl(1)	2.403(17)	Li(2)–N(2)	2.007(13)	K(0B)–N(1)cent	2.910(8)
Li–N(1)	2.020(2)	Li(1)–N(1)	2.066(2)	Li(2)–I(2)	2.851(12)	K(0B)n–N(2)cent	2.983(8)
Li–N(2A)	1.980(2)	Li(1)–O(1)	1.958(18)	Li(2)–O(2)	1.908(13)	K(0B)–O(1B)	2.675(8)
		Li(1)–O(2)	2.010(4)	Li(1A)–N(1)	2.011(12)		
		Li(2)–N(2)	2.074(17)	Li(1A)–O(1A)	1.922(12)		
		Li(2)–O(4)	1.985(19)	Li(1A)–I(1)	2.835(12)		
		Li(2)–Cl(2)	2.452(16)	Li(1A)–I(1A)	2.872(12)		
		Li(2)–Cl(2A)	2.457(16)				
Cl–Yb–N(1)cent	107.3(11)	Cl(1)–Yb–Cl(2)	99.5(8)	I(1)–Yb–N(1)cent	105.3(19)	N(1)–Yb–N(2)	93.4(2)
Cl–Yb–N(2)cent	106.5(11)	Cl(1)–Yb–N(1)cent	103.3(8)	I(1)–Yb–N(2)cent	109.8(19)	N(1)–Yb–N(1C)	117.8(2)
Cl–Yb–Cl(A)	87.63(11)	Cl(1)–Yb–N(2)cent	110.9(8)	I(1)–Yb–I(2)	92.9(15)	N(1)–Yb–N(2C)	115.0(2)
N(1)–Li–O(1)	110.4(11)	Cl(1)–Li(1)–N(1)	97.3(7)	I(2)–Li(2)–N(2)	98.2(5)	O(1B)–K(0B)–N(1)cent	110.5(17)
N(1)–Li–N(2A)	136.4(11)	Cl(1)–Li(1)–O(1)	101.0(8)	I(2)–Li(2)–O(2)	108.5(5)	O(1B)–K(0B)–N(2)cent	106.8(17)
		Cl(1)–Li(1)–O(2)	116.3(19)	O(2)–Li(2)–N(2)	122.2(6)		
		Cl(1)–Li(2)–Cl(2A)	94.1(6)	I(1)–Li(1A)–N(1)	98.6(5)		
		Cl(1)–Li(2)–N(2)	96.5(6)	I(1)–Li(1A)–O(1a)	106.9(5)		
		Cl(1)–Li(2)–O(4)	121.6(8)	I(1)–Li(1A)–I(1A)	103.8(4)		

^a cent denotes a bond length or angle calculated from the ring centroid.

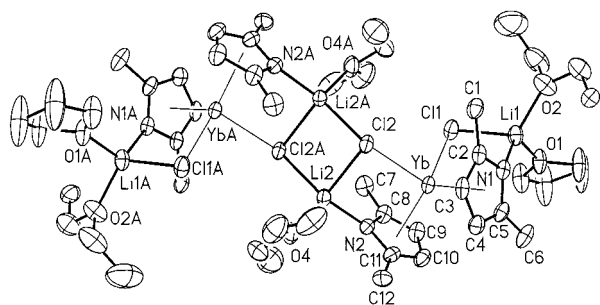


Figure 5. Thermal ellipsoid plot of **5**. Thermal ellipsoids are drawn at the 30% probability level.

of crystalline material from the reaction mother liquor, where **4** was still the major component. Since physical separation of the crystalline mass for analytical purposes proved unfeasible, an X-ray structure determination was the only possibility to identify complex **5**. Complex **5** (Figure 5) also has a dimeric structure that contains two divalent Yb atoms. Each unit contains an ytterbium atom that is π -bonded to two 2,5-dimethylpyrrole ligands (Yb–N(1)_{centroid} = 2.469(10) Å; Yb–N(2)_{centroid} = 2.54(10) Å) and σ -bonded to two chlorine atoms (Yb–Cl(1) = 2.682(3) Å; Yb–Cl(2) = 2.744(2) Å), providing a distorted-tetrahedral geometry around the ytterbium center. Each unit also contains two lithium atoms that are σ -bonded to a pyrrolide ligand (Li(1)–N(1) = 2.066(2) Å) and to a chlorine atom (Li(1)–Cl(1) = 2.403(17) Å). One of these lithium atoms is coordinated to two solvent molecules (one being THF and the other ether), while the second lithium atom is coordinated to a molecule of ether (Li(2)–O(4) = 1.985(19) Å) and a chlorine atom from the second unit (Li(2)–Cl(2A) = 2.452(16) Å), thus forming the dimeric structure. In its composition, complex **5** is very similar to complex **4**, except that it contains two additional LiCl units and four solvent molecules.

In analogy with the reactions described above, we have also reacted YbI₂(THF)₂ with 2 equiv of the lithium salt of 2,5-dimethylpyrrole in THF at room temperature. Red diamagnetic crystals of [(μ - η^1 : η^5 -Me₂C₄H₂N)₂Yb-

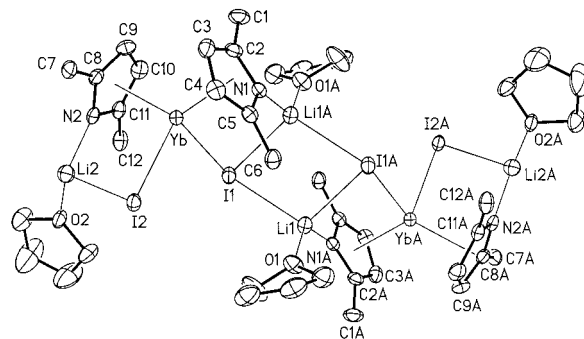


Figure 6. Thermal ellipsoid plot of **6**. Thermal ellipsoids are drawn at the 30% probability level.

(μ -I)₂[Li(THF)]₂(toluene)_n (**6**) were obtained from toluene after workup of the reaction mixture. Elemental analysis, ¹H NMR, and ¹³C NMR were in agreement with the structure elucidated by X-ray diffraction analysis (Figure 6). Complex **6** is very similar to **5**, the only difference arising from the nature of the halogen atom (iodine versus chlorine), thus reaffirming that halogens do not play a significant role in this chemistry. The divalent ytterbium atoms are still π -bonded by the pyrrolide ligands (Yb–N(1)_{centroid} = 2.440(7) Å; Yb–N(2)_{centroid} = 2.450(7) Å) and also σ -ligated to two iodine atoms (Yb–I(1) = 3.1203(5) Å; Yb–I(2) = 3.1174(5) Å), thus adopting a distorted-tetrahedral geometry. The only other noticeable difference between complexes **5** and **6** is that in the latter the ether molecules are partially replaced by THF. Each central lithium atoms bears two THF molecules (Li(1)–O(1) = 1.922(12) Å), while the terminal lithium is bonded to only one solvent molecule (Li(2)–O(2) = 1.908(13) Å).

To complete the series of experiments aimed at assessing the role of the alkali-metal cation in determining the structure and nuclearity of these complexes, we carried out the reaction of YbI₂(THF)₂ with 2 equiv of the potassium salt of 2,5-dimethylpyrrole in THF at room temperature. Yellow diamagnetic crystals of the divalent {(μ - η^1 : η^5 -Me₂C₄H₂N)₄[K(THF)₂Yb]}_n (**7**) were obtained from the reaction, which were characterized

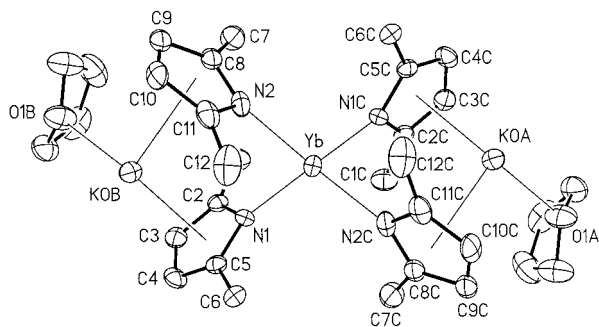


Figure 7. Thermal ellipsoid plot of **7**. Thermal ellipsoids are drawn at the 30% probability level.

as usual by elemental analysis, ^1H NMR, and ^{13}C NMR. The connectivity of **7** was elucidated by an X-ray structure determination (Figure 7). Complex **7** has a polymeric structure consisting of units that contain a single divalent ytterbium atom. The lanthanide metals are σ -bonded to four pyrrole ligands ($\text{Yb-N}(1) = 2.378(4)$; $\text{Yb-N}(1\text{C}) = 2.378(4)$; $\text{Yb-N}(2) = 2.409(4)$; $\text{Yb-N}(2\text{C}) = 2.409(4)$), which causes the metal to adopt a pseudo-tetrahedral geometry ($\text{N}(1)\text{-Yb-N}(2) = 93.4(2)^\circ$; $\text{N}(1)\text{-Yb-N}(2\text{C}) = 115.0(2)^\circ$; $\text{N}(1)\text{-Yb-N}(1\text{C}) = 117.8(2)^\circ$). The structure also contains two potassium atoms that are π -bonded to two pyrrole ligands ($\text{K}(\text{OB})\text{-N}(1)_{\text{centroid}} = 2.910(8) \text{ \AA}$; $\text{K}(\text{OB})\text{-N}(2)_{\text{centroid}} = 2.675(8) \text{ \AA}$) and also coordinated to a THF molecule ($\text{K}(\text{OB})\text{-O}(1\text{B}) = 2.675(5) \text{ \AA}$). The potassium atoms are responsible for the polymeric structure of **7**, as each atom is coordinated to a 2,5-dimethylpyrrole fragment, forming an infinite array.

The structure of **7** is a significant departure from the other structures reported in this work, once again emphasizing the remarkable role of the alkali-metal cation on both the structure and metal to ligand bonding mode. It is interesting to note that, as opposed to the structures described earlier, the pyrrole ligands in complex **7** coordinate the Yb center through σ -bonds instead of π -bonds.

Conclusions

By using the monopyrrole ligand 2,5-dimethylpyrrole, it was possible to synthesize and isolate a few novel divalent lanthanide complexes. From the data reported in this work, it seems reasonable to conclude that the bonding mode adopted by 2,5-dimethylpyrrole is likely directed not by the lanthanide metal or the solvent used but by the nature of the alkali metal. All the structures that include lithium atoms (complexes **1**, **2**, and **4–6**) have pyrrole fragments that exclusively form π -bonds to the Sm or Yb centers while the pyrrole nitrogen is σ -bonded to the lithium atom. The utilization of Na instead of Li, such as in complex **3**, causes samarium to be both π - and σ -bonded to the 2,5-dimethylpyrrole ligands, since the sodium atom is also bonded in a similar fashion. Finally, the presence of potassium, as in complex **7**, causes the lanthanide to form exclusively σ -interactions, since potassium in turn exclusively features π -interactions. Although the data reported in this work are not sufficient for a conclusive statistic, the indication that the bonding mode adopted by the lanthanide metal is entirely dependent on the nature of the alkali metal is very strong. A hard alkali-metal cation such as lithium is better stabilized by σ -bonding the ligand, which in turn confers π -bonding to the lanthanide center. A softer alkali metal such as potassium prefers to be π -bonded, which in turn leads to σ -bonded Sm or Yb centers.

Acknowledgment. This work was supported by the Natural Sciences and Engineering Council of Canada (NSERC).

Supporting Information Available: Listings of atomic coordinates, thermal parameters, and bond distances and angles for structures **1–7**. This material is available free of charge via the Internet at <http://pubs.acs.org>.

OM0109915